

4/6p.

N 65 - 35 205

FACILITY FORM 602

(ACCESSION NUMBER)	(THRU)
46	1
(PAGES)	(CODE)
TMX-54535	32
(NASA CR OR TMX OR AD NUMBER)	(CATEGORY)

(NASA TMX-54535)

THE PREDICTION OF NOTCH AND CRACK STRENGTH

UNDER STATIC OR FATIGUE LOADING

Paul Kuhn [1964] 46p ref 24

NASA Langley Research Center,  
Langley Station, Hampton, Va.

For presentation

Presented at the 1964 SAE-ASME National Air Transport  
and Space Meeting and Production Forum,

GPO PRICE \$ \_\_\_\_\_

CFSTI PRICE(S) \$ \_\_\_\_\_

Hard copy (HC) 2.00

Microfiche (MF) .50

conf.

ff 653 July 65

New York, New York  
April 27-30, 1964

unc-  
[REDACTED]  
[REDACTED]


THE PREDICTION OF NOTCH AND CRACK STRENGTH  
UNDER STATIC OR FATIGUE LOADING

By  
Paul Kuhn\*

To be presented at  
1964 SAE-ASME National Air Transport and  
Space Meeting and Production Forum.

April 27-30, New York

\*Assistant Chief, Structures Research Division, NASA Langley Research Center,  
Langley Station, Hampton, Virginia.



## INTRODUCTION

It is a well-known fact that service failures in structures usually originate at notches of some sort, particularly if the structure is subjected mainly to fatigue loading. In recognition of this fact, the better text books on strength of materials as long as thirty years ago contained a fair amount of information on theoretical stress concentration factors for various notches of practical interest, and a vast amount of additional information has become available since then.

However, tests and service experience showed consistently that the theoretical factors are almost always unduly conservative; not infrequently, experimental factors are an order of magnitude lower than the theoretical factors. Hundreds of experiments have been published, and constitute a large and confusing catalog of differences between theory and tests. Several reasons for the differences have been discussed, but in general, the discussions were essentially qualitative and did not result in the development of general methods for converting theoretical factors into factors suitable for use in design.

More recently, the effect of cracks on static strength has become a design problem. The sensitivity of materials to cracks varies greatly; in some materials, the static strength is reduced drastically by the presence of cracks. Airworthiness requirements for airplanes stipulate that a structure with cracks of specified length must develop a certain fraction of the strength required in the undamaged condition. In other types of structures, cracks due to fatigue or due to welding are a matter of vital concern. Adequate

methods for predicting the effect of cracks are therefore of great importance in all lines of structural engineering.

The present paper discusses a method of notch analysis intended to deal with notch problems in a unified manner. The development of the method has taken place in three main steps and is not considered completed. In the first step, a formula given by H. Neuber based on considerations of size effect was developed into a method for computing fatigue notch factors and was applied to parts made of low-alloy steels (ref. 1). In the second step, plasticity considerations were added which gave the capability of computing static strength factors for notches and cracks; extensive applications involving static as well as fatigue notch factors for wrought aluminum alloys were presented in reference 2. In the third step, the amplified method was applied to compute static strength factors for titanium alloy parts at cryogenic as well as elevated temperatures (ref. 3). The present paper has been prepared to summarize the current state of development of the method, to discuss its use in the field of testing of materials for notch strength, and to discuss two important extensions of the method.

SYMBOLS

APPEARING MORE THAN ONCE

B	Flow-restraint factor
E	Young's modulus, ksi
$E_1$	Secant modulus of elasticity pertaining to $\sigma_u$ , ksi
$K_T$	Theoretical factor of stress concentration
$K_N$	Factor of stress concentration, corrected for size effect; also predicted factor for notch fatigue at long life
$K_u$	Factor of stress concentration applicable to static fracture
$K_w$	Factor in formula (1)
R	Radius of cylinder, in.
$S_N$	Average stress on net section at static fracture (net section measured before loading begins)
a	Depth of edge notch, or half-length of transverse centerslot or crack, in.
b	Half-width of net section, in.
e	Elongation in 2-inch gage length
t	Thickness of specimen, in.
w	Width of specimen, in.
$\rho$	Radius of notch, in.
$\rho'$	Neuber constant, in.
$\sigma_{ty}$	Tensile yield strength (0.2% offset), ksi
$\sigma_u$	Tensile strength, ksi
$\omega$	Flank angle of notch, radians

## METHOD OF ANALYSIS

The method of notch analysis presented here is based on the conventional concept that a notched part will fail when the peak stress at the root of the notch becomes equal to the appropriate "allowable stress." The peak stress is calculated as the product of the net-section stress  $S_N$  and an appropriate factor of stress concentration. The first sub-section below outlines the procedure, while the later ones give the detailed formulas for notches (with finite radius) and for cracks. The discussion in this paper will be confined to flat symmetrical parts axially loaded except for fatigue.

### Outline of Procedure

Prediction of the static strength of a part with a finite-radius notch involves three main steps.

(a) The theoretical factor of stress concentration  $K_T$  is corrected for "size effect", which is ascribed to the granular structure of engineering alloys. Size effect is assumed to be governed by the "Neuber constant"  $\rho'$ . The corrected factor is denoted by  $K_N$ .

(b) The factor  $K_N$  is corrected for plasticity effect to obtain the final factor  $K_u$  for ultimate (static) strength. The correction is made by use of the ratio  $E_1/E$ , provided the net-section stress does not exceed the yield stress substantially. (The modified procedure for net-section stresses above the yield stress is discussed under "Notes on formulas").

(c) To obtain the "allowable stress", the tensile strength of the material is modified by an empirical factor  $(1 + B)$  which allows for the notch-strengthening due to restraint against flow at the root of the notch.

Step (c) is not involved in the calculation of the static strength of a cracked part, because notch strengthening is assumed to be negligible ( $B = 0$ ) for cracks, making the allowable stress equal to the tensile strength. Moreover, for cracks,  $K_T$  and  $K_N$  coalesce into one factor (ref. 2); thus, the final factor  $K_u$  takes the simple form given in formula (5).

For fatigue loading near the fatigue limit, only the first step (a) is involved; the factor  $K_N$  constitutes the predicted fatigue notch factor. The allowable stress in this case is the chosen fatigue stress.

#### Formulas for Notches With Finite Radius

The most important types of notches encountered on sheet parts are shown in figure 1. The formulas used are

$$K_T = 1 + 2 K_w \sqrt{\frac{a}{\rho}} \quad (1)$$

$$K_w = \sqrt{\frac{1 - \frac{2a}{w}}{1 + \frac{2a}{w}}} \quad (\text{internal notches}) \quad (1a)$$

$$K_w = 1 - \frac{2a}{w} \quad (\text{edge notches}) \quad (1b)$$

$$K_N = 1 + \frac{K_T - 1}{1 + \frac{\pi}{\pi - \omega_e} \sqrt{\frac{\rho'}{\rho}}} \quad (\omega_e = \frac{\omega}{2} \text{ for } \omega < \frac{2}{3} \pi) \quad (2)$$

( $\rho'$  from figure 2a, b or c or from special tests)

$$K_u = 1 + (K_N - 1) \frac{E_1}{E} \quad (S_N < \sigma_{ty}) \quad (3)$$

$$\frac{E_1}{E} \approx \frac{1}{1 + \frac{0.8eE}{\sigma_u}} \quad (3a)$$

$$S_N = \frac{\sigma_u}{K_u} (1 + B) \quad (B \text{ from figure 3}) \quad (4)$$

#### Formulas for Transverse Cracks

$$K_u = 1 + 2 K_w \sqrt{\frac{a}{\rho^3}} \frac{E_1}{E} \quad (S_N < \sigma_{ty}) \quad (5)$$

(Crack length is measured before load is applied)

(Note approximation for  $\frac{E_1}{E}$  given by formula (3a))

$$S_N = \frac{\sigma_u}{K_u} \quad (6)$$

#### Notes on Formulas

(a) All applications to either static or fatigue strength predictions should conform to the restrictions noted in figures 2(a) and 2(c) and at the end of the section "Determination of Neuber Constants."

(b) Formula (2) is general; it applies, for instance, to circular or elliptical holes and filleted shoulders as well as to the notches shown in figure 1.

(c) For sheet containing center slots or cracks, the value of  $S_N$  calculated by expression (4) or (6) should be multiplied by the correction factor

$$\left(1 - 0.001 \frac{2a}{t}\right) \quad (7)$$



to allow for buckling along the edges of the crack. Material tests should preferably be run with guides to suppress this buckling, at least when  $2a > 50t$ , since the correction factor is not well substantiated.

(d) Recent results suggest that the quantity  $E_1/E$  in formulas (3) and (5) should be replaced by  $E_1/\sqrt{EE_N}$  when  $S_N > \sigma_{ty}$  (more precisely, when  $S_N$  exceeds the proportional limit).

(e) The factor  $K_w$  in formulas (1a) and (1b) is based chiefly on photo-elastic tests in references 4 and 5.

(f) The empirical quantity  $B$  in formula (4) is subject to considerable scatter. The factor  $K_T$  is probably not an adequate parameter for defining  $B$ .

#### DISCUSSION OF METHOD

Two aspects of the method warrant discussion. One is the problem of determining the Neuber constants, which may be regarded as the foundation of the method. The other is the much-discussed question of relationships between notch-sensitivity and other material properties, which will be examined briefly in the light of the method of notch analysis.

#### Determination of Neuber Constants

The Neuber constant  $\rho'$  for a given material can be determined either from fatigue tests or from static tests. Nominally, a Neuber constant is intended only to define "size effect", that is, it establishes an "effective stress" value and has no relation to fracture characteristics. However, the possibility exists that the experimentally determined  $\rho'$ -values may reflect to some extent fracture characteristics and thus may depend on the type of test from which they are derived - fatigue or static test.

For aluminum alloys, extensive experimental evidence was found in the literature for notch fatigue as well as for static notch strength of sheet material, and it was found that the  $\rho'$ -values given by figure 2(b) represent both types of tests equally well. It has also been found that the relationship between  $\rho'$  and  $\sigma_u$  shown in figure 2(b) apparently does not change when the test temperatures are lowered to cryogenic values. (This does not mean that  $\rho'$  is independent of temperature, since  $\sigma_u$  changes with temperature.)

For low-alloy steels, a wealth of literature exists on notch fatigue, but practically no tests have been made on notch strength of sheet material. The  $\rho'$ -curve of figure 2(a) is therefore based entirely on fatigue tests.

There has been, of course, much work done on the fracture of mild steel in plate form. The behavior of thick plate is more difficult to assess than that of thin sheet. Moreover, investigations on the behavior of plate material have concentrated heavily on such properties as transition temperatures and impact energy, while tensile strength and elongation were largely disregarded. An analysis of these tests by means of the present method is therefore severely handicapped by paucity of useable data and has not been attempted.

On titanium sheet material, there has been a large amount of work in the last few years to determine tensile strength and notch strength, engendered by the good characteristics which some of the alloys offer for various applications in aerospace engineering. Consequently, it has been possible to develop tentative  $\rho'$ -curves as shown in figure 2c. They are regarded as tentative because a large portion of the test data on which they are based were obtained on material produced at a time when production techniques were

not too well stabilized. The available information on the notch strength of titanium covers temperatures ranging from  $-423^{\circ}$  F to over  $600^{\circ}$  F. On the basis of this information, it appears that the  $\rho'-\sigma_u$  relation given by figure 2(c) is valid for all temperatures within the range quoted, which is obviously a highly important observation.

While the current situation regarding test information on the static notch strength of titanium is fairly good, the situation regarding notch fatigue strength is bad. The experimental information is quite limited, a substantial part of it is highly specialized, some of it is falsified by test difficulties that were not recognized at the time, and finally much of it was obtained at a time when the manufacturing technology was still beset by development troubles. Whatever the detailed reasons may be, a preliminary survey shows that there appears to be no hope of devising a system for predicting notch fatigue factors for titanium alloys until a reasonable quantity of better data is obtained.

On stainless steels, some information on crack strength is available (ref. 6), and more is being obtained. Stainless steels vary greatly in chemistry, cold work, and heat treatments, with the result that there is a large variety of characteristics. It must be presumed, therefore, that plots of  $\rho'$  would not show one or two curves as in figures 2(a), (b), or (c), but a large number of curves, some of which might be rather short. For the time being, it does not seem possible to do more than tabulate such  $\rho'$ -values as may be obtained.

Notch fatigue information on stainless steels is too sparse at present to permit any deductions.

The review given in this section shows that the applicability of one given set of  $\rho'$ -values to the calculation of static as well as fatigue notch factors has been demonstrated so far only for the aluminum alloys. Prudence dictates, therefore, that the application of  $\rho'$ -values for other materials be restricted, for the time being, to the type of tests - fatigue or static - from which they were derived. The curves of figures 2a and 2c are therefore labeled accordingly.

#### Relations Between Notch Sensitivity and Other Material Properties

The formulas presented make it possible to compute notch factors, provided certain materials properties are known. There is considerable controversy about the relations between notch sensitivity and other material properties. In particular, the old school of thought holds that elongation is a fairly direct index of notch sensitivity, while one new school holds that elongation has nothing to do with notch sensitivity and consequently does not even report elongation values in elaborate investigations on notch sensitivity. It seems worthwhile, therefore, to examine briefly how the method of notch analysis views this matter.

Fatigue notch factors are computed by formula (2), which contains the Neuber constant  $\rho'$  and no other material property. Thus, according to this method, the fatigue notch sensitivity of a material is characterized fully by  $\rho'$ .

For certain classes of materials, the constant  $\rho'$  is related to the tensile strength  $\sigma_u$  by a curve. Thus, for materials within one such class, comparative rankings of fatigue notch sensitivity could be based on the tensile strength.

Static crack strength factors are computed by formula (5), with the possibility of using the approximation given by formula (3a). Thus, the method of notch analysis contends that the static crack sensitivity of a material can be characterized either by the quantity  $\sqrt{\rho'} E/E_1$  or by the quantity  $\sqrt{\rho'} (1 + \frac{0.8eE}{\sigma_u})$ . The latter contains explicitly the permanent elongation  $e$ , while the former contains the uniform elongation implicitly in the modulus  $E_1$ . If the term "elongation" is used in a general sense to include either one, the following statements may be made:

(a) Elongation alone is not sufficient to characterize static crack sensitivity, since it appears in the formula in combination with several other material properties.

(b) Elongation must be known (in one form or another) to completely characterize static crack sensitivity if "conventional" tensile properties ( $E$  and  $\sigma_u$ ) are used to characterize it (and  $\rho'$  must also be known).

The last statement implies that the value of a number of research investigations has been greatly reduced by failure to report elongation values.

The static strength of parts with finite-radius notches is affected by the same parameters as the crack-strength and, in addition, by notch-strengthening. Since the amount of notch-strengthening is a function of the geometry of the part (fig. 3), it appears that static notch sensitivity (particularly for mild notches) cannot be considered as a pure materials property.

## EXPERIMENTAL VERIFICATION

In the development of the method, strong emphasis has been placed on extensive experimental verification. Since rather full coverage is given in the references, only samples have been chosen for presentation here. Some indications have been given of the accuracy of prediction that may be expected. However, because of the large scope of the method, it is difficult to be specific on this score, and the potential user of the method should study the data and form his own opinions.

### Low-Alloy Steels

Figure 4 shows sample predictions (from ref. 1) of fatigue notch factors for rotating shafts with filleted shoulders. Each of the three test series represents a group of specimens of varying size, but geometrically similar and consequently having the same value of  $K_T$ . For two groups, the agreement between test and prediction is practically perfect; for the third group, there is a discrepancy of about ten percent. These results are reasonably typical of those obtained for a large variety of specimen types and materials; the total number of test points analyzed to date is about 300, with about 260 presented in reference 1. The prediction error is within  $\pm 20\%$  for 84% of the tests.

### Aluminum Alloys

Reference 2 presents first about 160 sets of fatigue tests on aluminum-alloy specimens, 90 of which are for axially loaded specimens while the rest are rotating beams. Over-all, the prediction error is within  $\pm 20\%$  for 77% of the tests; however, counting only axially loaded specimens, 20% accuracy or better is achieved for 85% of the specimens.

Reference 2 next presents a large series of static crack-strength test results from a number of laboratories on sheet specimens with transverse cracks or fine saw-cuts. Specimens vary in width from 2.25 to 35 inches and include a variety of alloys, without and with cladding. Also shown are a number of results on plate and bar specimens.

For the sheet specimens, no coupon data were available for most tests. Predictions were therefore made on the basis of typical material properties taken from the material manufacturer's handbooks. The predictions were generally quite close (conservative in a few cases for short cracks) for copper alloys. On the only zinc-alloy (7075-T6), there was considerably more scatter evident, and some unconservative predictions resulted when typical elongations were used as basis for prediction; however, no significantly unconservative predictions were obtained when specification minimum elongations were used as basis for calculation.

Reference 2 shows rather conservative predictions for some low-strength alloys, for which the net-section stresses at failure were well above the yield stress. However, close predictions result if the procedure given as Item (d) under "Notes on Formulas" in the present paper is used.

Figure 5 shows results from a set of crack-strength tests conducted by an aircraft firm in England (ref. 7), thus affording a check of the method for a number of alloys not included in the tests evaluated in reference 2. The specimens were sheets, either 10 or 30 inches wide, with central fatigue cracks. Three tensile coupon tests were made for each material, and the predicted

curves shown as full lines were calculated on the basis of these coupon properties. For the zinc-alloys, additional calculations were made - shown as dashed curves - based on elongations taken from reference 8. This modification of procedure is roughly equivalent to the use of minimum elongation mentioned above for the 7075-T6 specimens in reference 2.

It may be noted in figure 5 that the test points at  $2a/w = 0.7$  are substantially lower than predicted for some materials. No explanation can be suggested for this discrepancy.

Figures 6 and 7 (from ref. 2) represent data which are felt to have a special significance. The specimens are of rectangular configuration with central transverse fatigue cracks, but they are substantially thicker than all the other specimens in reference 2 and those of figure 5. The results shown in figure 5 are for plates 0.25 inch thick (machined from 1-inch plate), while those in figure 7 are for bars 0.75 inch thick. Both figures show rather good agreement between test and prediction. This agreement implies that there is no "thickness effect" exhibited by these specimens, a result which is remarkable in view of a wide-spread belief that important thickness effects may be found well within the range of sheet gages (thickness less than one-quarter inch).

Figures 8(a) and 8(b) show comparisons taken from reference 3 for a series of tests made at Watertown Arsenal (ref. 9). The specimens, as noted, are Vee-notch specimens 0.64 inch wide, with a notch radius of 0.002 inch. The experimental values of tensile strength and elongation are shown for information and the curves connecting these points are simply faired



through the test points; the curves for notch-strength ratio, however, are calculated. Even at the cryogenic test temperatures, there is reasonably good agreement between test and prediction, indicating that the  $\rho'$ -curve of figure 2(b) may be used within the temperature range of these tests and possibly lower.

#### Titanium Alloys

Figure 9 shows comparisons (taken from ref. 3) for sets of test data on titanium alloys taken from reference 10. The specimen in this case is one recommended by the ASTM (ref. 11), a Vee-notch specimen one-inch wide with a notch radius of 0.0007 inch. It will be noted that the test temperatures range from  $-110^{\circ}$  F to  $+650^{\circ}$  F. The rather good agreement between test and calculated notch-strength ratios for all alloys indicates that the  $\rho'$ -curve of figure 2(c) may be used over this temperature range. Other tests extending to  $-423^{\circ}$  F are unfortunately less completely reported, but indicate that the  $\rho'$ -curves may be used down to liquid-hydrogen temperatures.

### APPLICATIONS TO NOTCH TENSILE TESTING

#### General Remarks

For the purpose of discussion here, the term "notch-tensile testing" will be defined as applying to tensile tests on sheet-type specimens of symmetrical shape, not employing impact loading. This definition excludes a large number of tests which are widely used, but it still encompasses a large variety of specimen sizes and types actually used. This variety exists because consideration must be given to

- (a) desired accuracy of determining notch sensitivity
- (b) amount of material available
- (c) capacity of testing machine available
- (d) cost of specimens and tests

and possibly other factors. The last three considerations are self-explanatory and generally favor the use of small specimens. Unfortunately, the first consideration runs strongly counter to this. Small specimens (say one inch wide) are very "insensitive" to rather large changes in notch sensitivity; thus, they may be adequate in preliminary screening tests for sorting out materials with objectionably high notch sensitivity, but they are often unable to define differences between materials in the desirable range of low notch sensitivity. For the purpose of obtaining final design data, the aircraft industry has made extensive use of specimens 35 inches wide, but this width is obviously not acceptable economically for exploratory work. In practice, specimen widths anywhere between 0.6 inch and 36 inches have been used, and standardization on a single width appears to be quite impractical.

The notch sharpness also varies greatly in practice. For machined notches, theoretical factors may be as high as 20 and as low as 3 or less; for cracks, the theoretical factors are indefinitely large. Since cracks constitute the main problem encountered in actual structures, there appears to be little justification for employing machined notches to simulate cracks other than the fact that machine shops are not commonly equipped with fatigue machines. This situation can be remedied by procuring a simple type of fatigue machine, and there is an increasing tendency to use specimens with cracks

rather than with machined notches. In the meantime, however, thousands of tests have been made with machined notches and constitute the largest part of the information published at the present time.

In preliminary design, the engineer may thus find himself frequently confronted with the task of comparing results obtained with different types of specimens. Such comparisons can be accomplished by notch analysis, and the following sections will give indicative examples. Comparative calculations based on estimated properties can also be used as aid in choosing specimen configuration for a contemplated test series in a more rational manner than by a sketchy experimental investigation or by arbitrary selection.

#### First Example (Effect of Notch Radius)

The first example has been chosen to demonstrate that even a very small radius may not simulate a crack in a notch-sensitive material. The example also shows how notch-analysis can be used to determine whether tests on specimens with cracks or with finite-radius notches are consistent with each other or not.

The test data were taken from reference 11. The material was H-11 (mod.) tool steel; the specimens were one inch wide and had either Vee-notches or cracks 0.15 in. deep on each edge. Figure 10 shows experimental values of the notch-strength ratio plotted against the square root of the radius. Inspection of the test points shows that a 4-mil radius gives a notch strength about 4 times larger than a crack, and a 1-mil radius still gives a notch strength about twice as large as a crack. Thus, radii in this range are

much too large to simulate a crack. On the 0.6 mil radius, the scatter suggests that the machining was probably out of control.

Most conventional methods of notch-testing use only a go-no go criterion of correlation: the Vee-notch either is sufficiently acute to simulate a crack, or it is not. In this case, none of the Vee-notches are sufficiently acute, and no correlation between them and the specimens with cracks can be established.

Notch analysis was now applied as follows. The notch-strength ratios for the cracked specimens were averaged (point A, fig. 10), and the result was used to compute the Neuber constant. Next, utilizing this value of  $\rho'$ , notch-strength ratios were computed for Vee-notch specimens. Two curves are shown, computed for  $e = 8\%$  and  $e = 10\%$ , respectively, because the elongation had to be estimated from information given in reference 12, no coupon values being reported. Inspection of the figure shows that the test points for Vee-notch specimens with radii of 2, 3, and 4 mils agree very well with the computed curves. This means that the results obtained with 2, 3, and 4 mil radius specimens are consistent with those obtained from the cracked specimens.

The notch strengths of the 1-mil radius specimens are somewhat lower than predicted, while the average of the 0.6-mil radius specimens is very low. Since this group of specimens with the smallest radius in addition shows much more scatter than any other group, the most logical procedure probably would be to discard these three measurements.

### Second Example (Effect of Specimen Width)

For the second example, three sets of tests on sheet specimens with cracks were chosen from reference 2 to cover as large a range of width as possible. The data plots are shown in figure 11. The specimens with  $w = 35$  inches and  $w = 12$  inches had center cracks, while the specimens with  $w = 2.25$  inches had edge cracks; this difference in crack location has a slight effect on the direct comparison of the stresses, but has no effect on comparisons between tests and calculations.

Comparison of the experimental stresses for a given ratio  $2a/w$ , say 0.3 shows that  $S_N$  increases from about 33 ksi (for  $w = 35$ ) to about 54 ksi (for  $w = 2.25$  in.), an increase of over 60 percent. Moreover, the stresses for the narrow specimens are above the yield stress ( $\sigma_{ty} = 50$  ksi).

Predictions by the method of notch analysis are shown as dashed curves for the "guided" condition (buckling prevented by guide plates) and as full-line curves for the "unguided" condition. (For the  $w = 2.25$  in. specimens, the two conditions are considered to be identical.) All tests except one (solid point) are without guides; thus, test points should be compared with the full-line curve, excepting the solid point. The predictions were based on typical material properties ( $\sigma_u$ ;  $e$ ; and  $E$ ) taken from reference 13, supplemented by a typical stress-strain curve needed for the calculations for the 2.25-inch specimens because  $S_N$  here exceeds the yield stress. Inspection of figure 11 shows that the predictions made by notch-analysis are slightly conservative and quite consistent for all three widths.

Figure 11 also shows curves fitted to the test points of each set by the

$K_c$ -method of reference 11. It may be seen that it was necessary to assume a different value of  $K_c$  for each width of specimen in order to fit the test points, indicating that the  $K_c$ -formulas do not make proper allowance for changing width of specimens. The value of  $K_c$  for the 35-inch specimens is 75% larger than for the 2.25-inch specimens and thus can hardly be considered a materials "constant". It may be noted that the calculations were made using the "plastic-zone correction"; when this correction is not used (a practice followed by some engineers), the discrepancy is much larger.

#### EXTENSIONS OF METHOD

Since notch analysis is intended to be used for the strength analysis of complete structures, extensions are necessary to deal with more complex cases than the simple sheet.

One extension deals with a sheet containing a crack or slot which is bridged by a stiffener. A theoretical correction factor (ref. 14) reduces this case, in effect, to the case of a simple crack or slot of equivalent length. Details of the method and experimental verification are given in reference 15; a summary plot showing experimental points and predicted curves is given in figure 12. The problem is of considerable practical importance, because skin fatigue cracks often originate at a connection with a stiffener.

Another extension permits application of the method to a longitudinal crack in a pressure vessel of radius  $R$ . The formula used is

$$K_{uCYL} = K_u \left( 1 + 5 \frac{2a}{R} \right) \quad (8)$$

where  $K_u$  is the value calculated for the configuration which results when

the cylinder is "unrolled" into a flat configuration after cutting it longitudinally along a line diametrically opposite to the crack. This formula was derived from tests on aluminum-alloy cylinders (ref. 16); its applicability to other materials has not yet been verified. Figure 13 shows an application to bursting tests on cracked cylinders at cryogenic temperature, with test data taken from reference 17.\*

#### CONCLUDING REMARKS

The method of notch analysis presented here has demonstrated the capability of predicting fatigue notch factors as well as static strength notch factors, utilizing as basis conventional tensile properties and a "Neuber constant".

For low-alloy steels, wrought aluminum alloys and titanium alloys, Neuber constants have been defined by curves and may thus be regarded as known. For aluminum alloys, it has been shown that the Neuber constants may be used to compute either fatigue or static notch factors. At present, Neuber constants for low-alloy steels may be used only for fatigue notch strength calculations, while the constants for titanium alloys may be used only for static notch strength calculations. Additional research is needed to determine whether the constants for low-alloy steels and for titanium alloys can be used in the same general manner as for aluminum alloys.

---

\*In reference 16, the values of  $K_u$  were not computed by the present method of notch analysis; re-analysis of the tests using the present method resulted in changing the empirical constant from the value of 4.6 to the value of 5 given in formula (8).

For stainless steels, successful applications to the problem of static notch strength have been made, but the Neuber constants must be obtained for these materials on an individual basis.

The method of notch analysis is intended chiefly for use in fatigue design and in the strength analysis of structures containing cracks. It permits greatly increased utilization of the existing store of information on notch strength and crack strength of materials, because it affords reliable comparisons between tests made on specimens of widely different widths and with different types of notches. It also aids in making a more rational choice of specimens for notch testing and will permit a great reduction in this type of testing.

The scope of the method has been greatly extended by formulas which make it applicable to cylinders and to stiffened sheet.

One line of desirable additional research has been mentioned above. Another one is the problem of static notch strength of thick sections in all materials. Methods for taking strain-rate effects into account should be developed, and correlation with transition-temperature data should be established to round out the picture.



REFERENCES

1. Kuhn, Paul, and Hardrath, Herbert F.: An Engineering Method for Estimating Notch-Size Effect in Fatigue Tests on Steel. NACA TN 2805, 1952.
2. Kuhn, Paul, and Figge, I. E.: Unified Notch-Strength Analysis for Wrought Aluminum Alloys. NASA TN D-1259, 1962.
3. Kuhn, Paul: Notch Effects on Fatigue and Static Strength. ICAF-AGARD Symposium on Aeronautical Fatigue, Rome, Italy, April 1963.
4. Dixon, J. R.: Stress Distribution Around a Central Crack in a Plate Loaded in Tension; Effect of Finite Width of Plate. J. Roy. Aero. Soc., March 1962.
5. Dixon, J. R.: Stress Distribution Around Edge Slits in a Plate Loaded in Tension. J. Roy. Aero. Soc., May 1962.
6. Figge, I. E.: Residual Static Strength of Several Titanium and Stainless-Steel Alloys and One Super-Alloy at  $-109^{\circ}$  F,  $70^{\circ}$  F, and  $550^{\circ}$  F. NASA TN D-2045.
7. Harpur, N. F.: Material Selection for Crack Resistance. Crack Propagation Symposium, Cranfield, England, September 1961.
8. Anon: Material Properties Handbook, Vol. I Aluminum Alloys. North Atlantic Treaty Organization, Advisory Group for Aeronautical Research and Development.
9. Hickey, Charles F.: Mechanical Properties of Titanium and Aluminum Alloys at Cryogenic Temperatures. ASTM Preprint 78, 1962.

10. Raring, Richard H., Freeman, J. W., Schultz, J. W., and Voorhees, H. R.:  
Progress Report of the NASA Special Committee on Materials Research  
for Supersonic Transports. Part I - Committee Activities. Part II -  
Results of Supersonic Transport Materials Screening Program. NASA  
TN D-1798, 1963.
11. Anon.: Fracture Testing of High-Strength Sheet Materials. A Report of  
a Special ASTM Committee. Materials Research and Standards Bulletin,  
ASTM.
  - (a) First Report, chapter I, January 1960
  - (b) First Report, chapter II, February 1960
  - (c) Third Report, November 1961.
12. Anon.: Properties and Selection of Materials. Metals Handbook, vol. 1,  
8th edition, published by American Society for Metals, 1961.
13. Anon.: Alcoa Aluminum Handbook. Aluminum Company of America, 1959.
14. Sanders, J. Lyell: Effect of a Stringer on the Stress Concentration  
Due to a Crack in a Thin Sheet. NASA TR R-13, 1959.
15. Leybold, H. A.: A Method of Predicting the Strength of a Stiffened  
Sheet Containing A Sharp Central Notch. NASA TN D-1943, Aug. 1963.
16. Peters, Roger W., and Kuhn, Paul: Bursting Strength of Unstiffened  
Pressure Cylinders With Slits. NACA TN 3993, 1957.
17. Getz, Pierce and Calvert: Correlation of Uniaxial Notch Tensile Data  
With Pressure Vessel Burst Characteristics. ASME Preprint 63WAl87,  
Nov. 1963.

## FIGURE TITLES

Figure 1. - Standard types of notches used in notch-sensitivity tests on sheet materials. (Uniaxial tensile loading.)

Figure 2. - Neuber constants.

(a) Neuber constants for low-alloy steels. (From ref. 1)

Note: Use only for fatigue notch factors.

(b) Neuber constants for wrought aluminum alloys. (From ref. 2;

T = Heat-treated; O = Annealed; H = Strain-hardened.)

(c) Tentative Neuber constants for titanium alloys.

Note: Use only for static notch factors.

Figure 3. - Flow-restraint parameters for sheet-metal parts of aluminum or titanium alloys (use only when  $b/t \geq 4$ ).

Figure 4. - Experimental and predicted notch-fatigue factors for low-alloy steel rotating beams with shoulders. (From ref. 1.)

Figure 5. - Experimental and predicted failing stresses for cracked aluminum-alloy sheet. Data from reference 7.

Figure 6. - Experimental and predicted failing stresses for aluminum-alloy plate with center cracks. ( $w = 7.5$  in.;  $t = 0.25$  in.; from ref. 2.)

Figure 7. - Experimental and predicted failing stresses for aluminum-alloy bar with center cracks. ( $w = 2$  in.;  $t = 0.75$  in.; from ref. 2.)

Figure 8. - Tensile strengths, elongations, and notch-strength ratios of aluminum-alloy sheet as function of test temperature. Full-line curves are calculated. Specimen  $w = 0.64$  in.;  $45^\circ$  Vee-notch;  $a = 0.1$  in.;  $\rho = 0.002$  in. Data from reference 9.

Figure 9. - Tensile strengths, elongations, and notch-strength ratios of titanium-alloy sheet as function of test temperature. Full-line curves are calculated. Specimen  $w = 1.0$  in.;  $60^\circ$  Vee-notch;  $a = 0.15$  in.;  $\rho = 0.0007$  in. Data from reference 10.

Figure 10. - Notch-strength ratio of H-11 (mod.) tool steel as function of notch radius. Data from reference 11.

Figure 11. - Crack strength of 2024-T3 aluminum-alloy sheet specimens compared with notch-analysis predictions and  $K_c$  fitted curves.

Figure 12. - Experimental and predicted failing loads on slotted sheets with stiffeners bridging slots. Data from reference 15.

Figure 13. - Experimental and predicted bursting stresses on cracked 2014-T6 cylinders. Test data from reference 17.

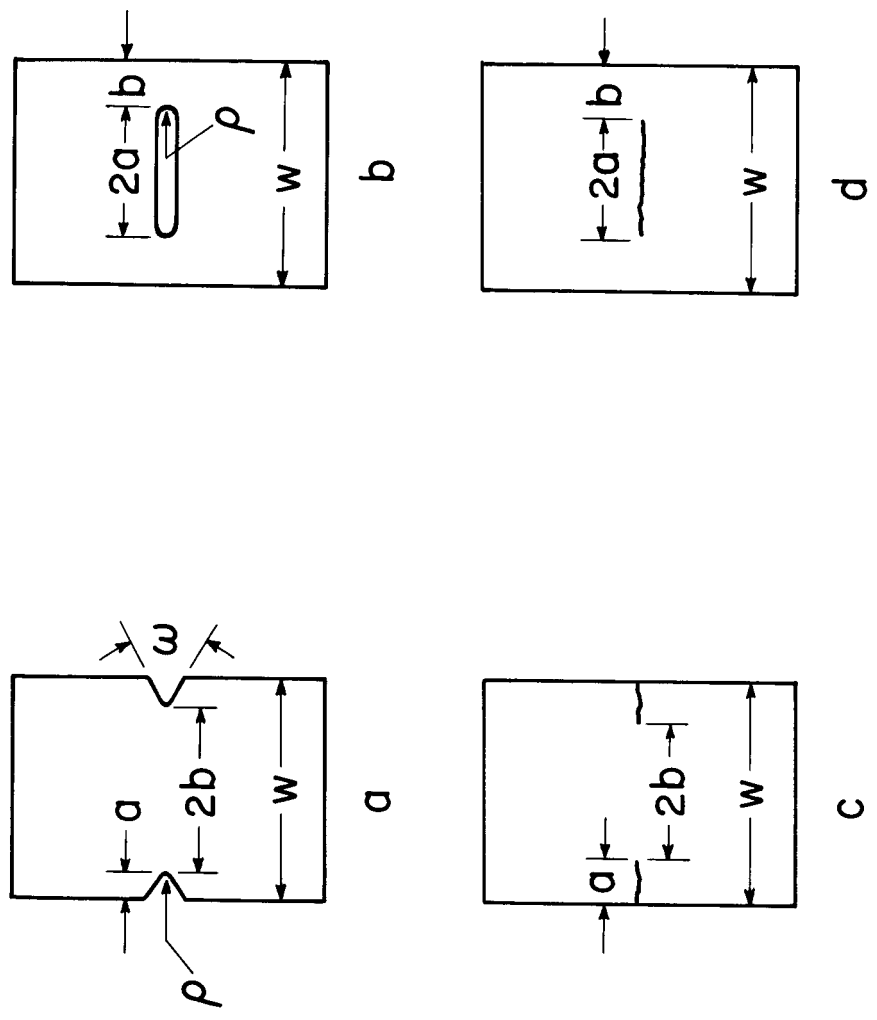
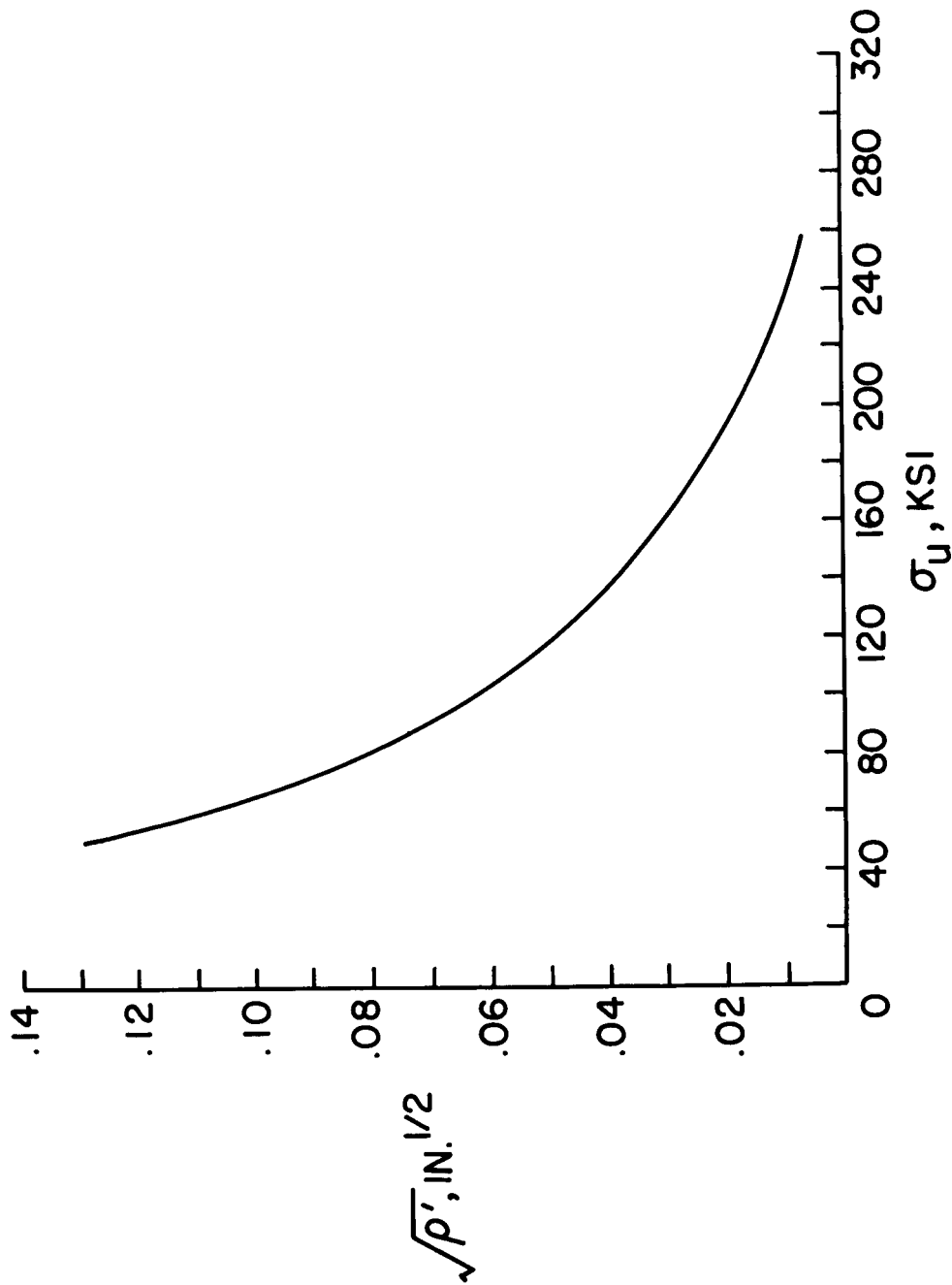
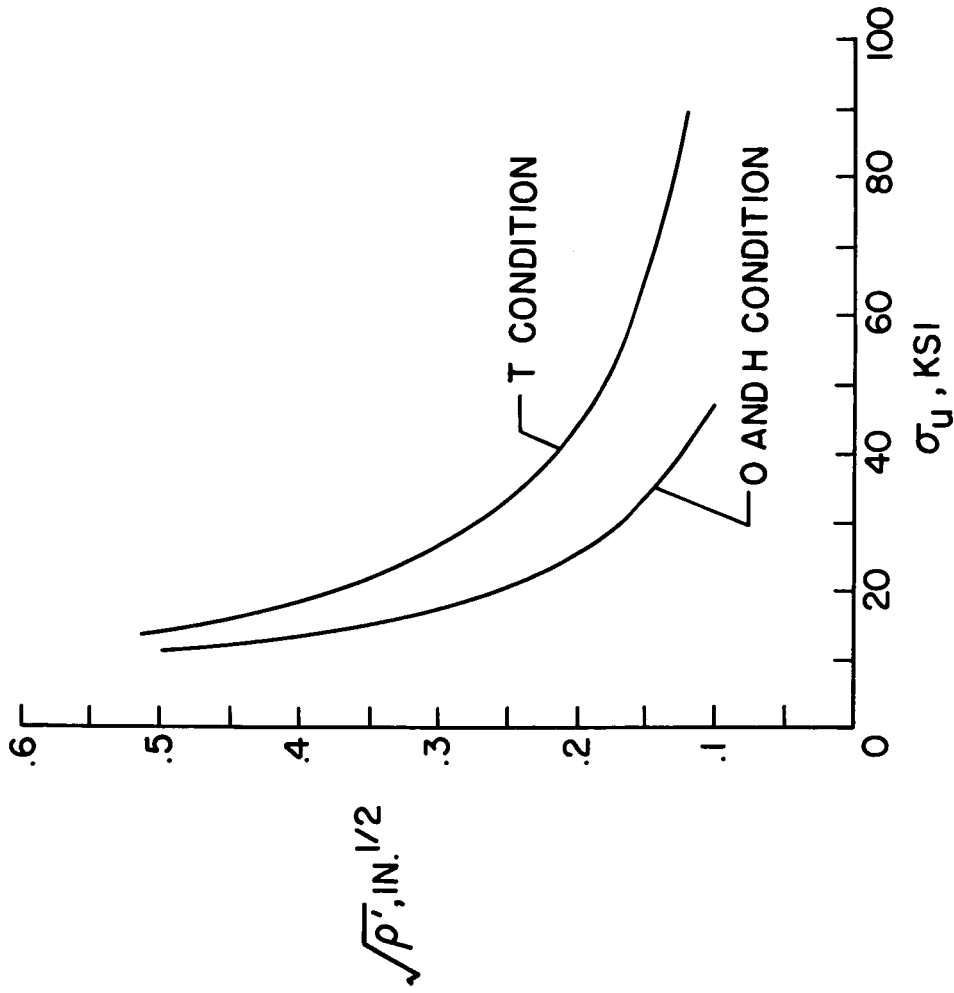


Figure 1.-- Standard types of notches used in notch-sensitivity tests on sheet materials. (Uni-axial tensile loading.)



(a) Neuber constants for low-alloy steels. (From ref. 1) Note: Use only for fatigue notch factors. NASA

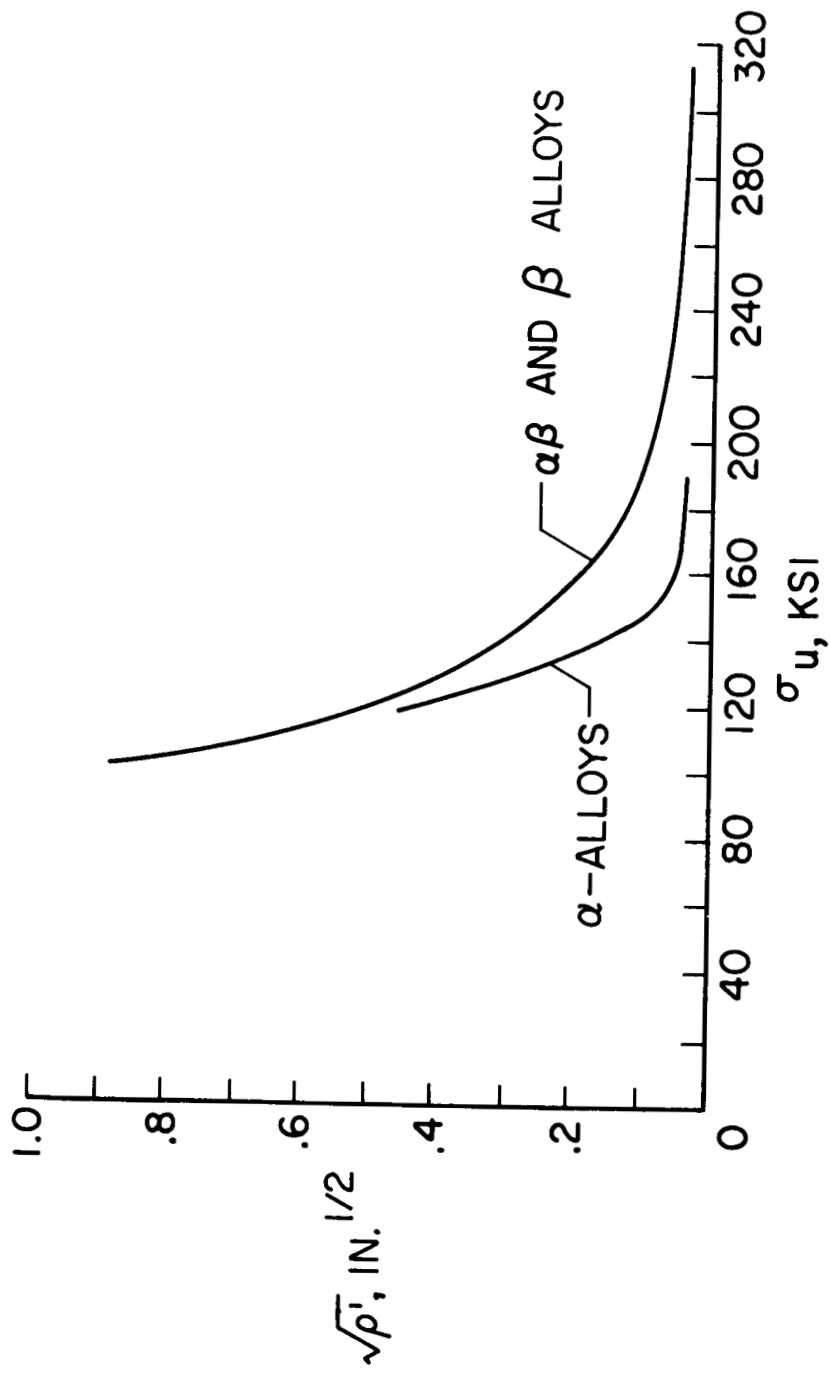
Figure 2.- Neuber constants.



NASA

(b) Neuber constants for wrought aluminum alloys. (From ref. 2; T = Heat-treated; O = Annealed; H = Strain-hardened.)

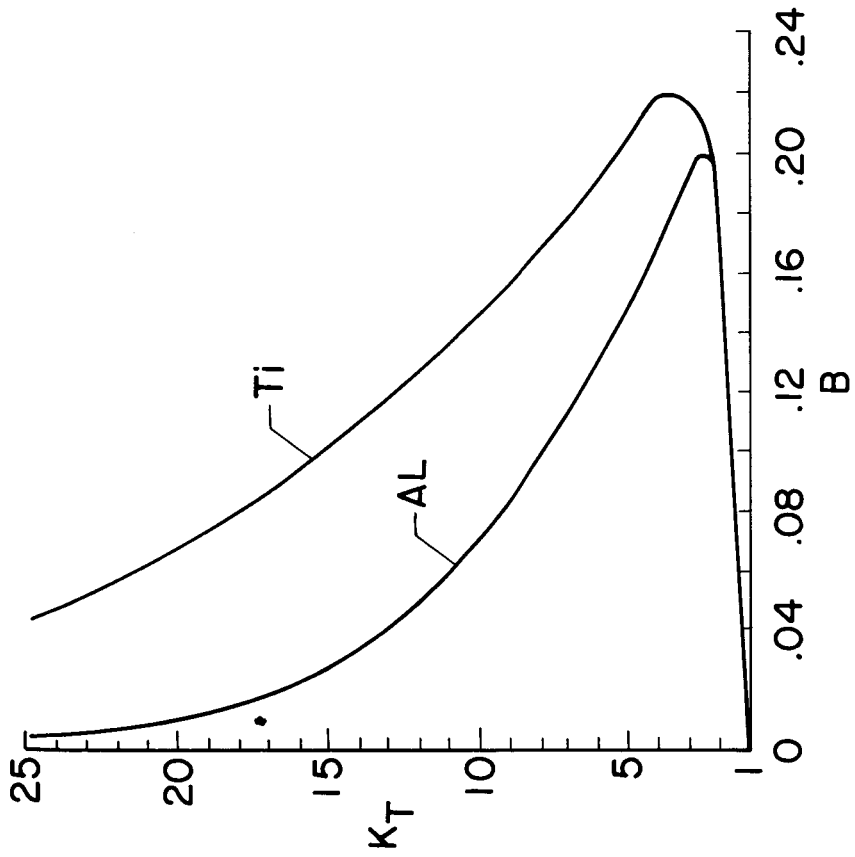
Figure 2.- Continued.



(c) Tentative Neuber constants for titanium alloys. Note: Use only for static notch factors. NASA

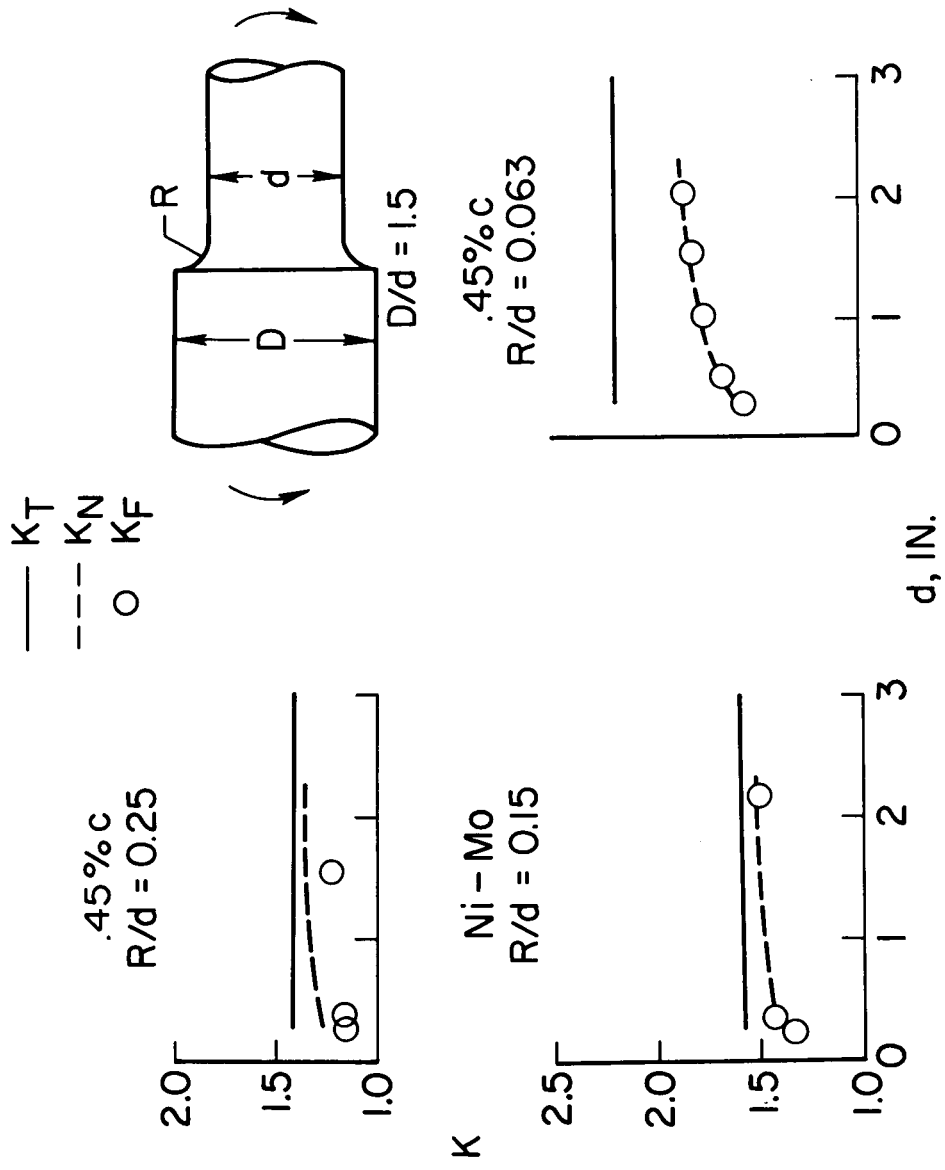
Figure 2.- Concluded.





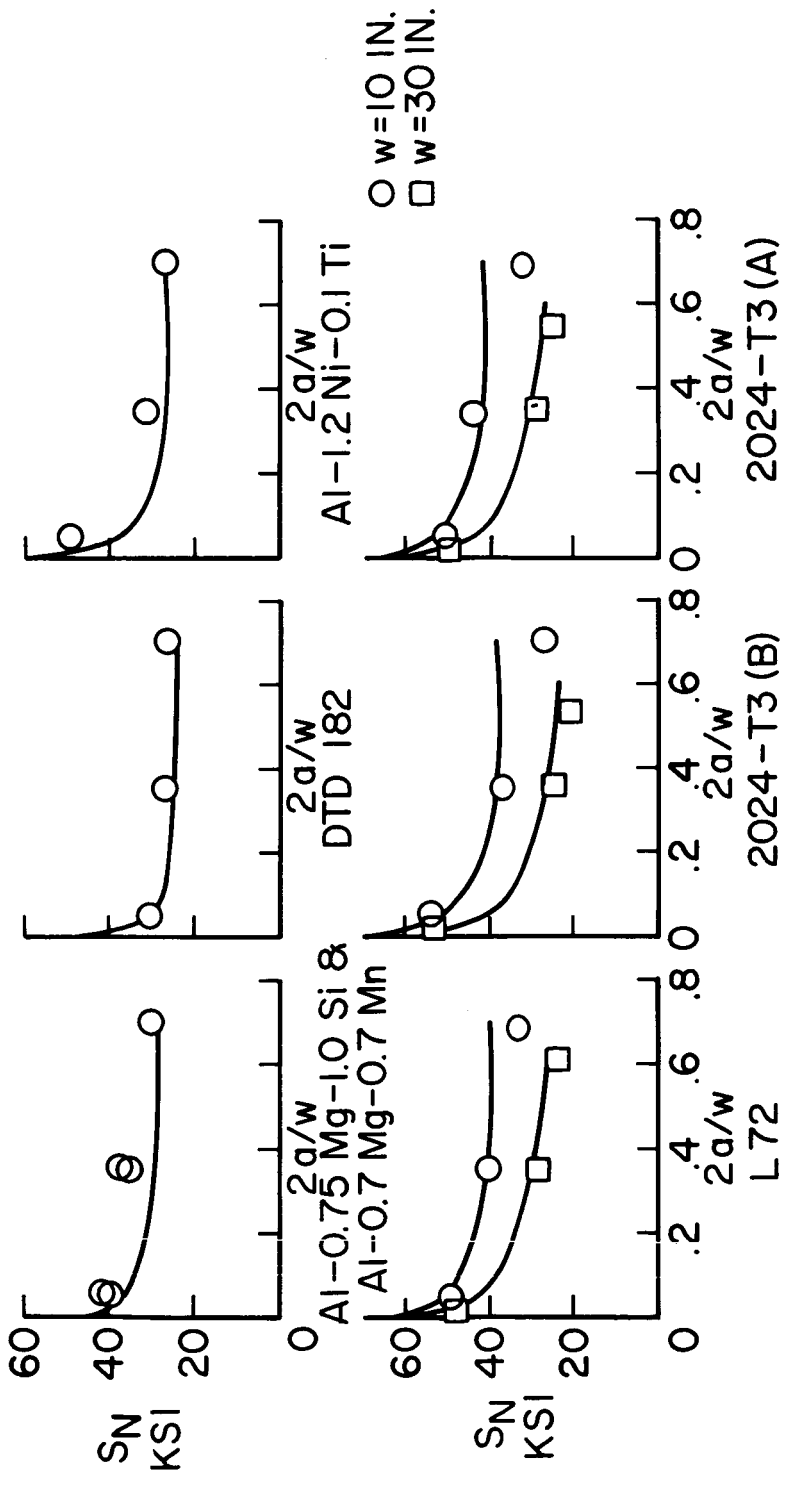
NASA

Figure 3.- Flow-restraint parameters for sheet-metal parts of aluminum or titanium alloys (use only when  $b/t > 4$ ).



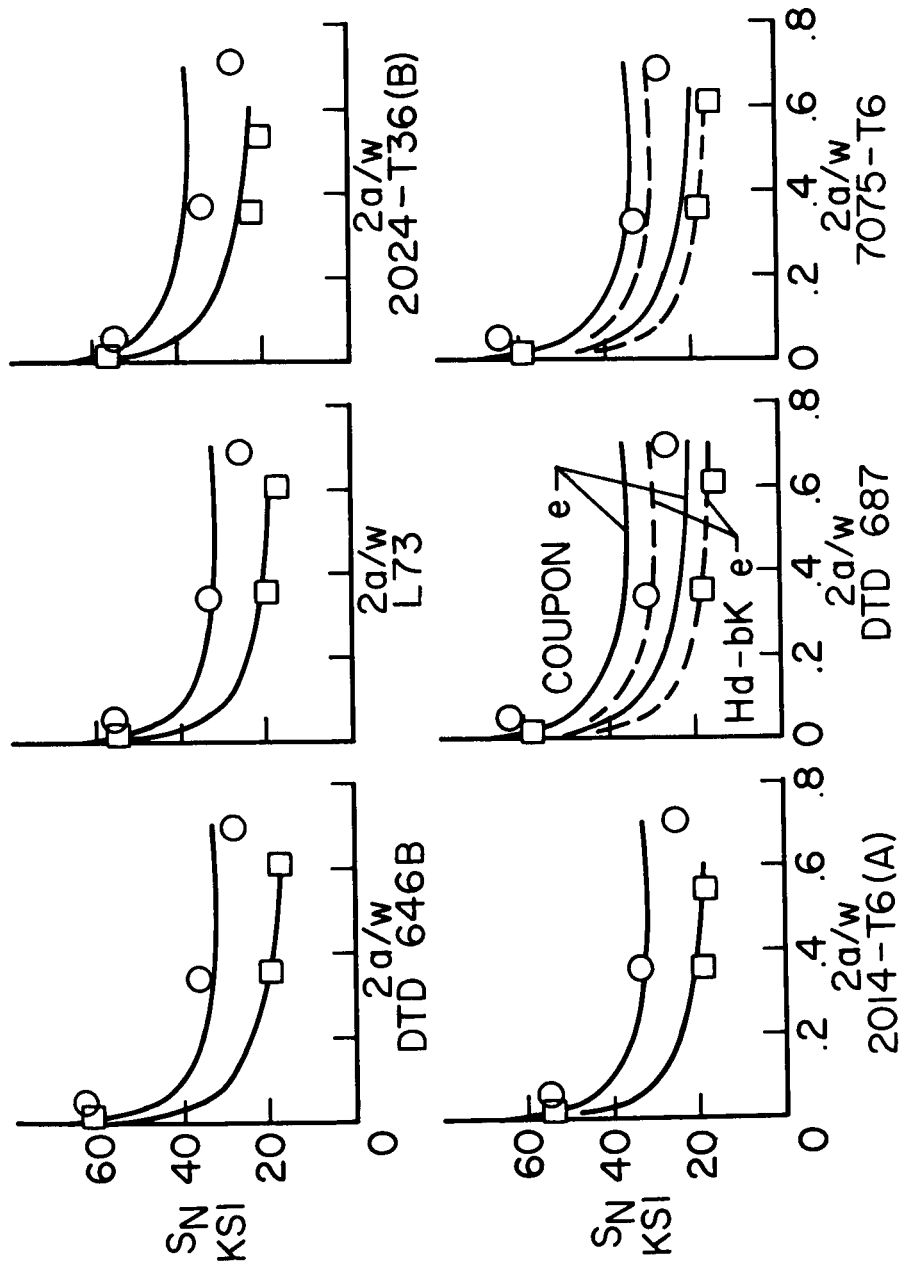
NASA

Figure 4.- Experimental and predicted notch-fatigue factors for low-alloy steel rotating beams with shoulders. (From ref. 1.)



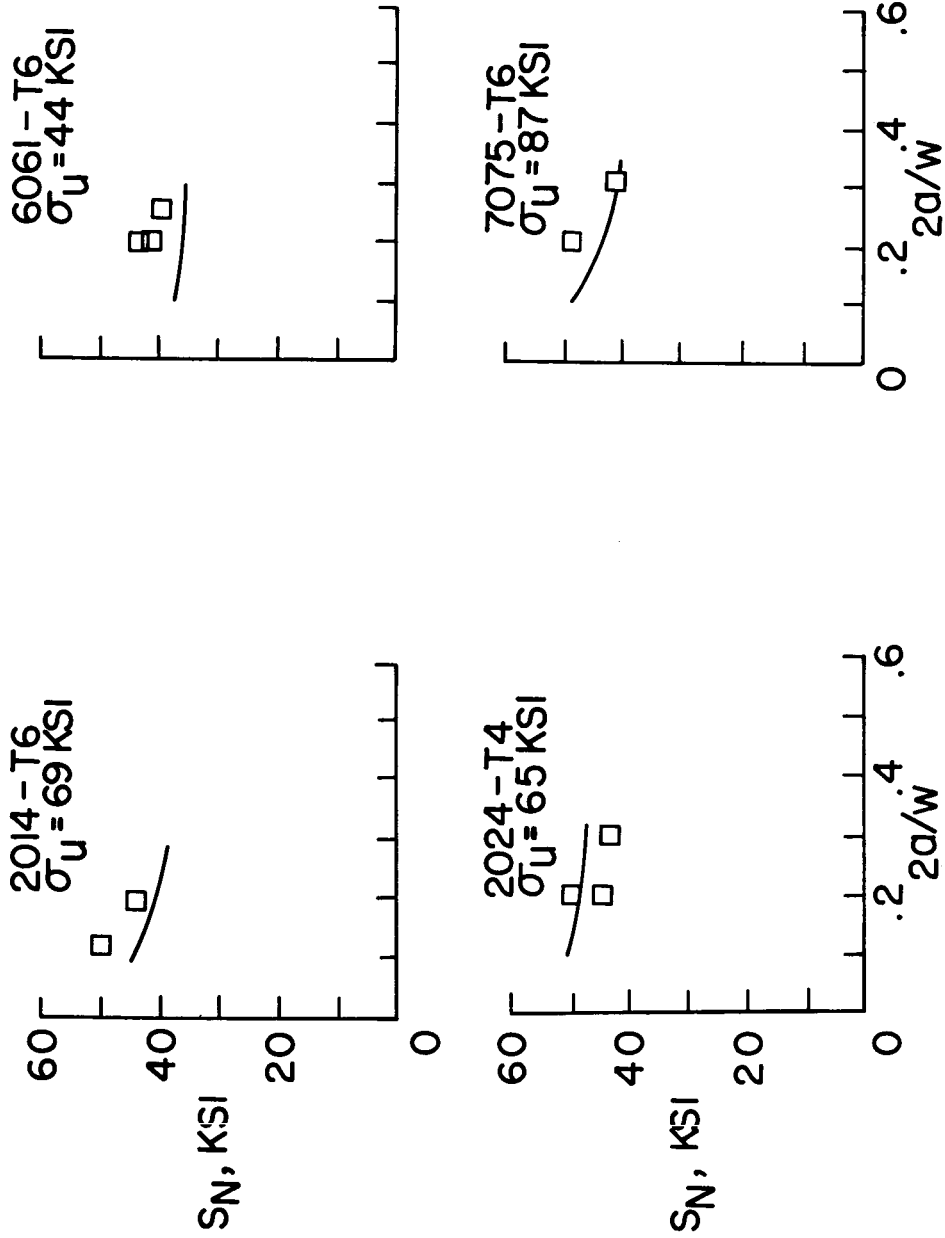
NASA

Figure 5.- Experimental and predicted failing stresses for cracked aluminum-alloy sheet. Data from reference 7.



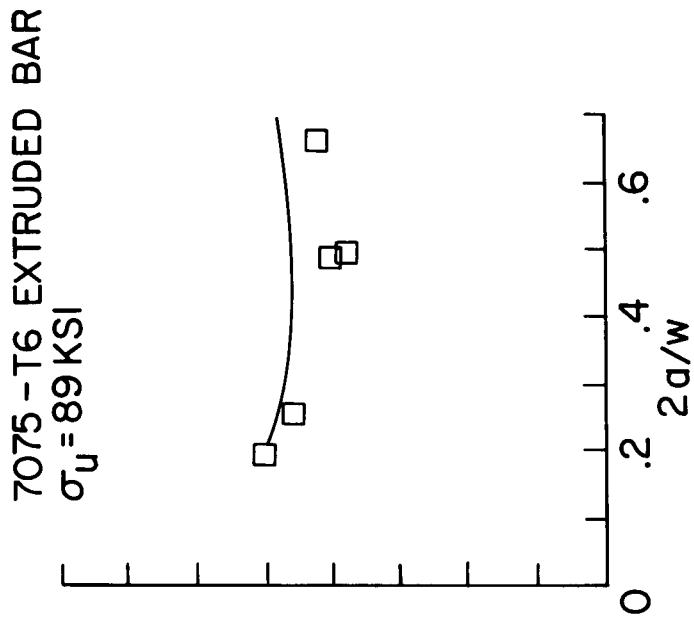
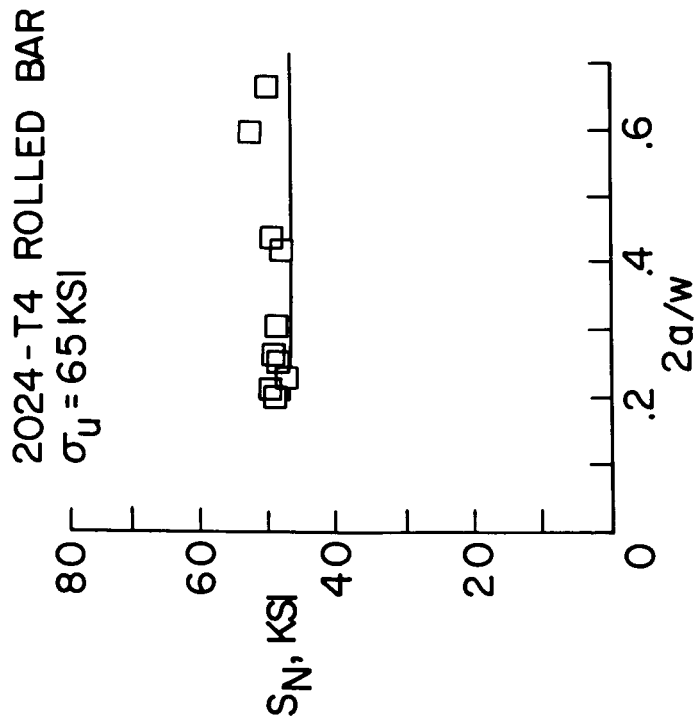
NASA

Figure 5.- Concluded.



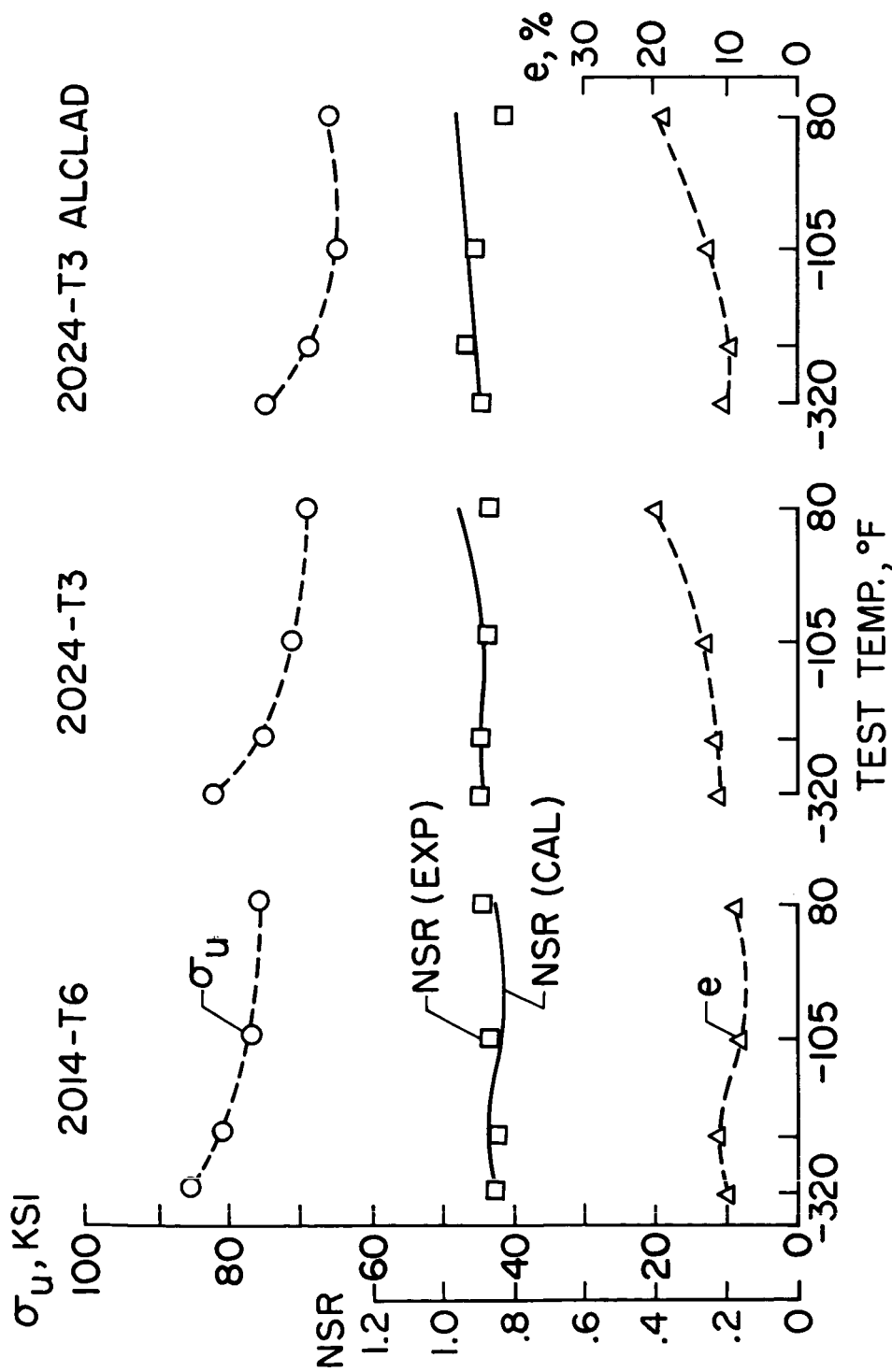
NASA

Figure 6.- Experimental and predicted failing stresses for aluminum-alloy plate with center cracks. ( $w = 7.5$  in.;  $t = 0.25$  in.; from ref. 2.)



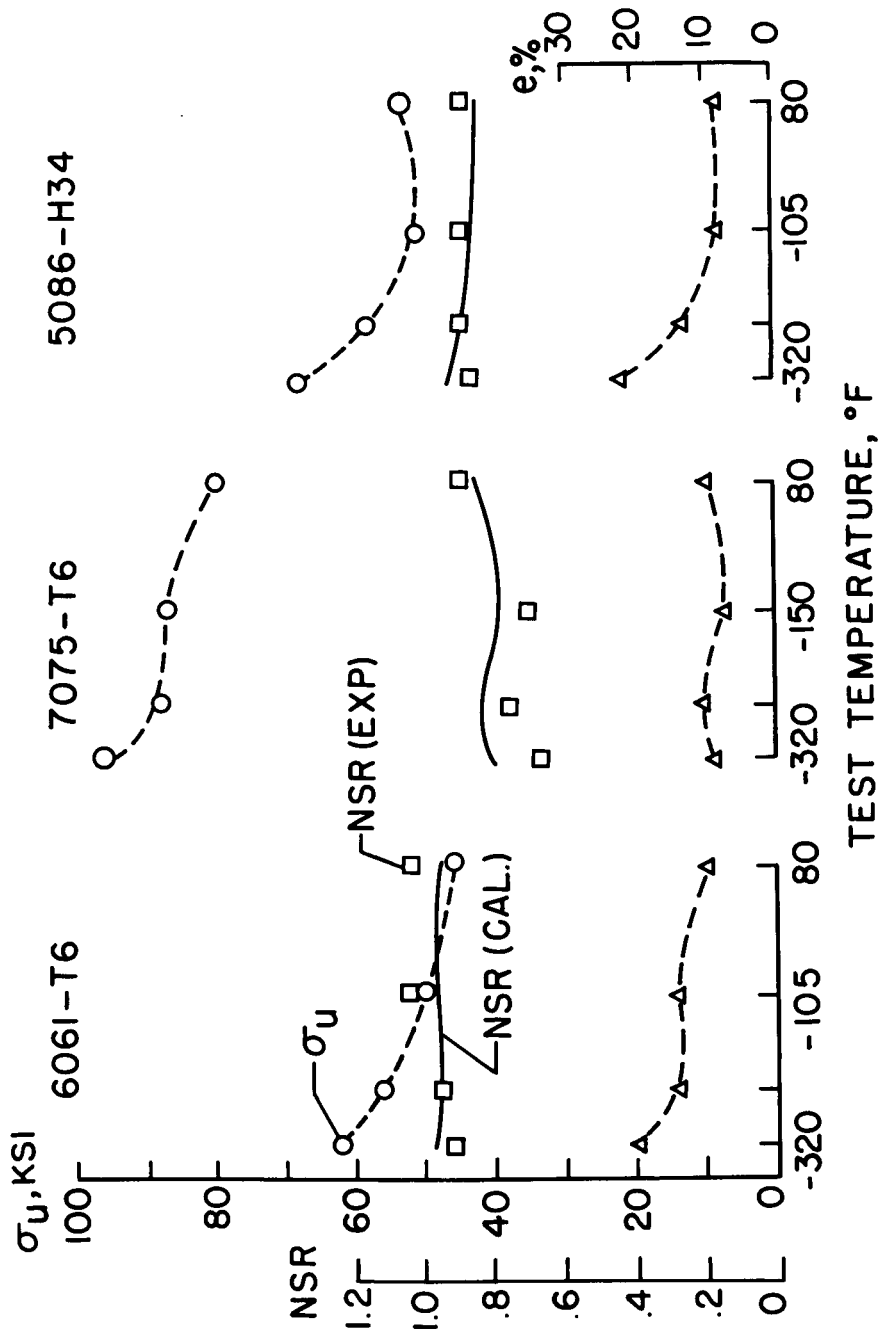
NASA

Figure 7.- Experimental and predicted failing stresses for aluminum-alloy bar with center cracks.  
 ( $w = 2 \text{ in.}$ ;  $t = 0.75 \text{ in.}$ ; from ref. 2.)



NASA

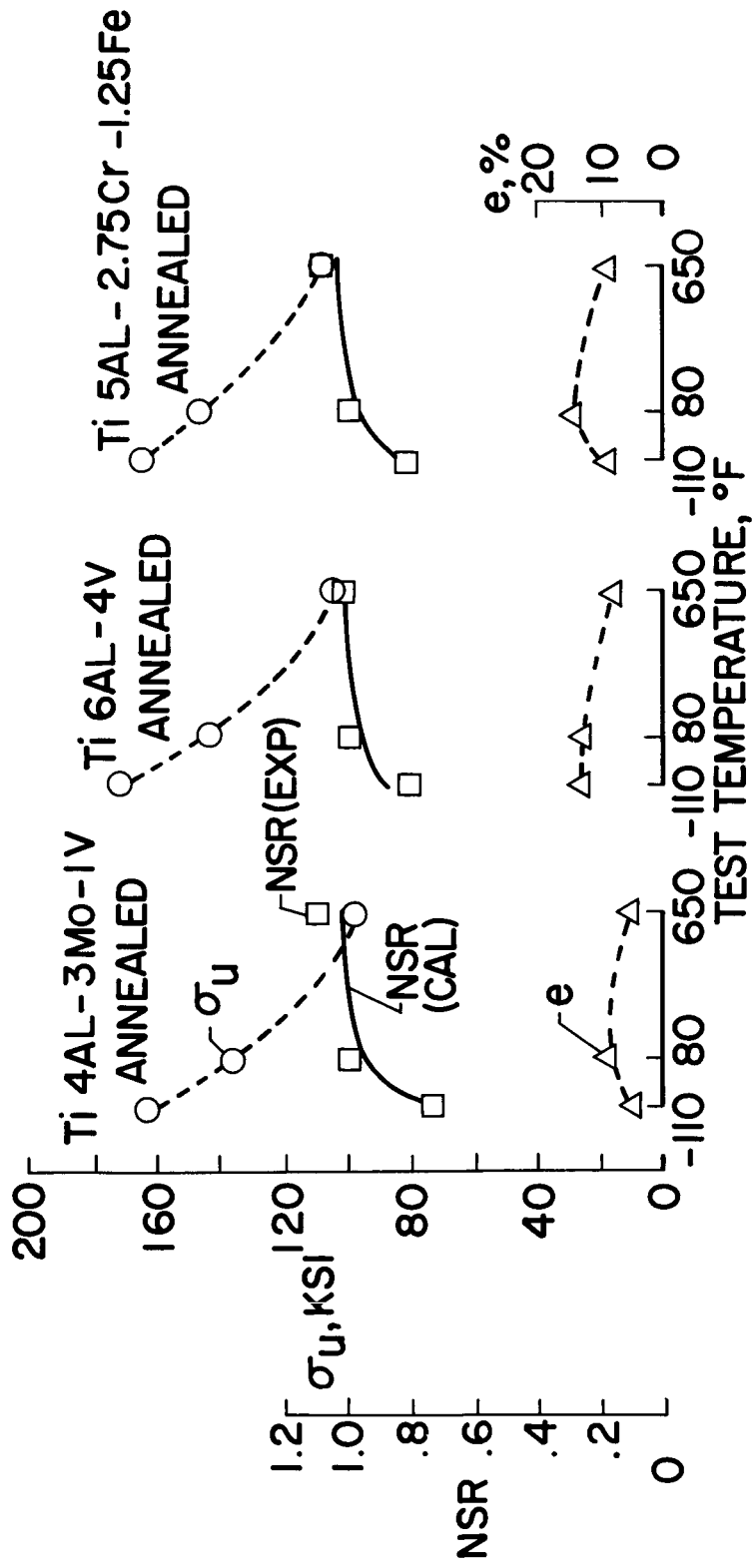
Figure 8.- Tensile strengths, elongations, and notch-strength ratios of aluminum-alloy sheet as function of test temperature. Full-line curves are calculated. Specimen  $w \approx 0.64$  in.;  $45^\circ$  Vee-notch;  $a \approx 0.1$  in.;  $\rho = 0.002$  in. Data from reference 9.



NASA

Figure 8.- Concluded.





NASA

Figure 9.- Tensile strengths, elongations, and notch-strength ratios of titanium-alloy sheet as function of test temperature. Full-line curves are calculated. Specimen  $w = 1.0$  in.;  $60^\circ$  Vee-notch;  $a = 0.15$  in.;  $\rho = 0.0007$  in. Data from reference 10.

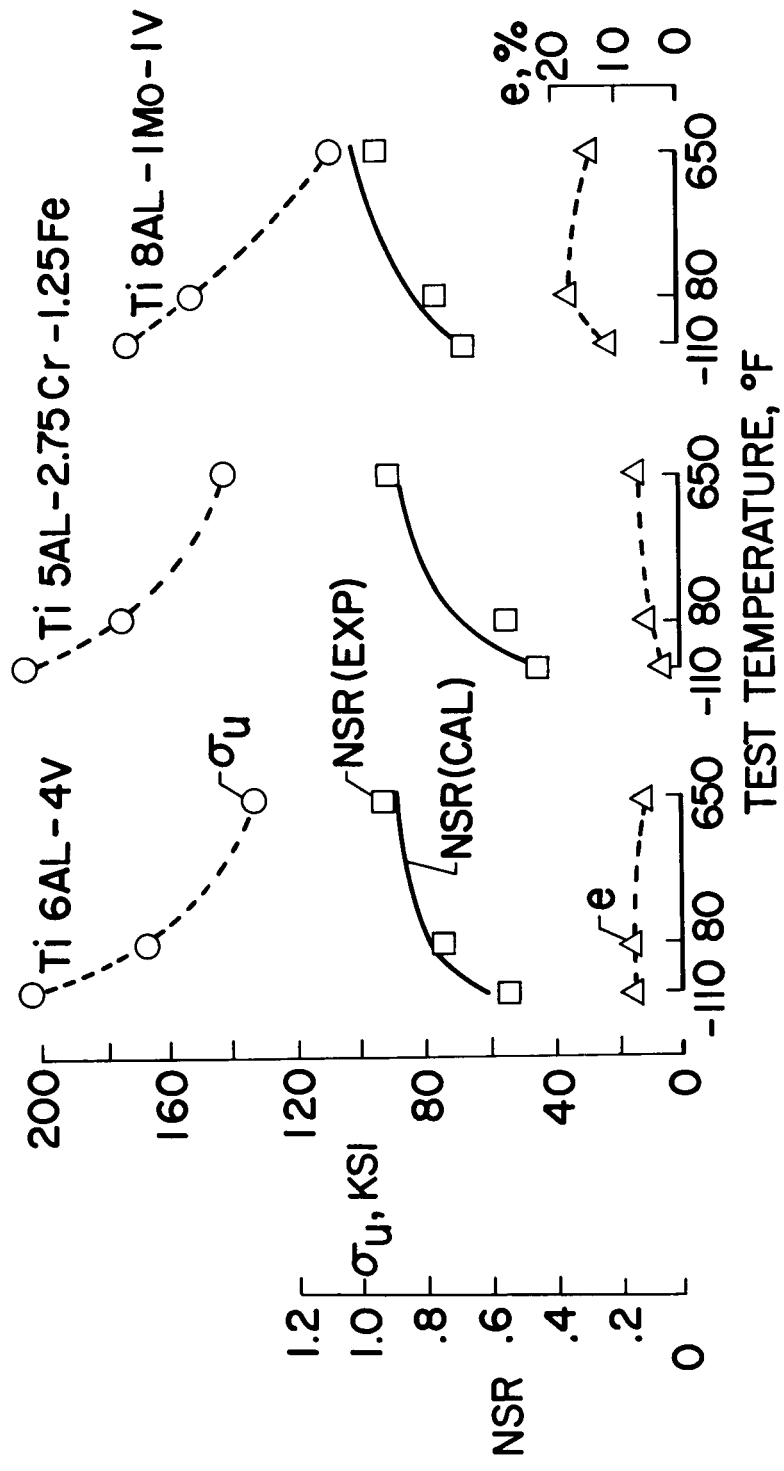


Figure 9.- Concluded

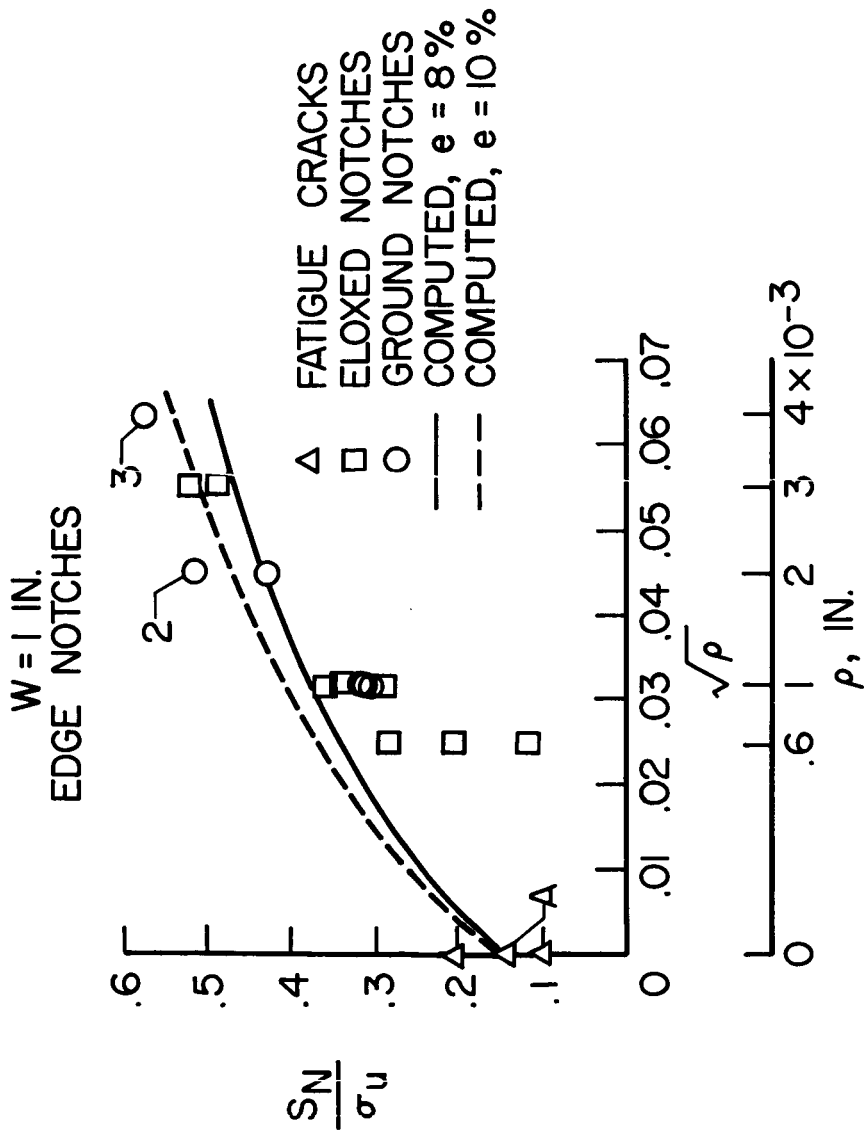


Figure 10.- Notch-strength ratio of H-11 (mod.) tool steel as function of notch radius. Data from reference 11.

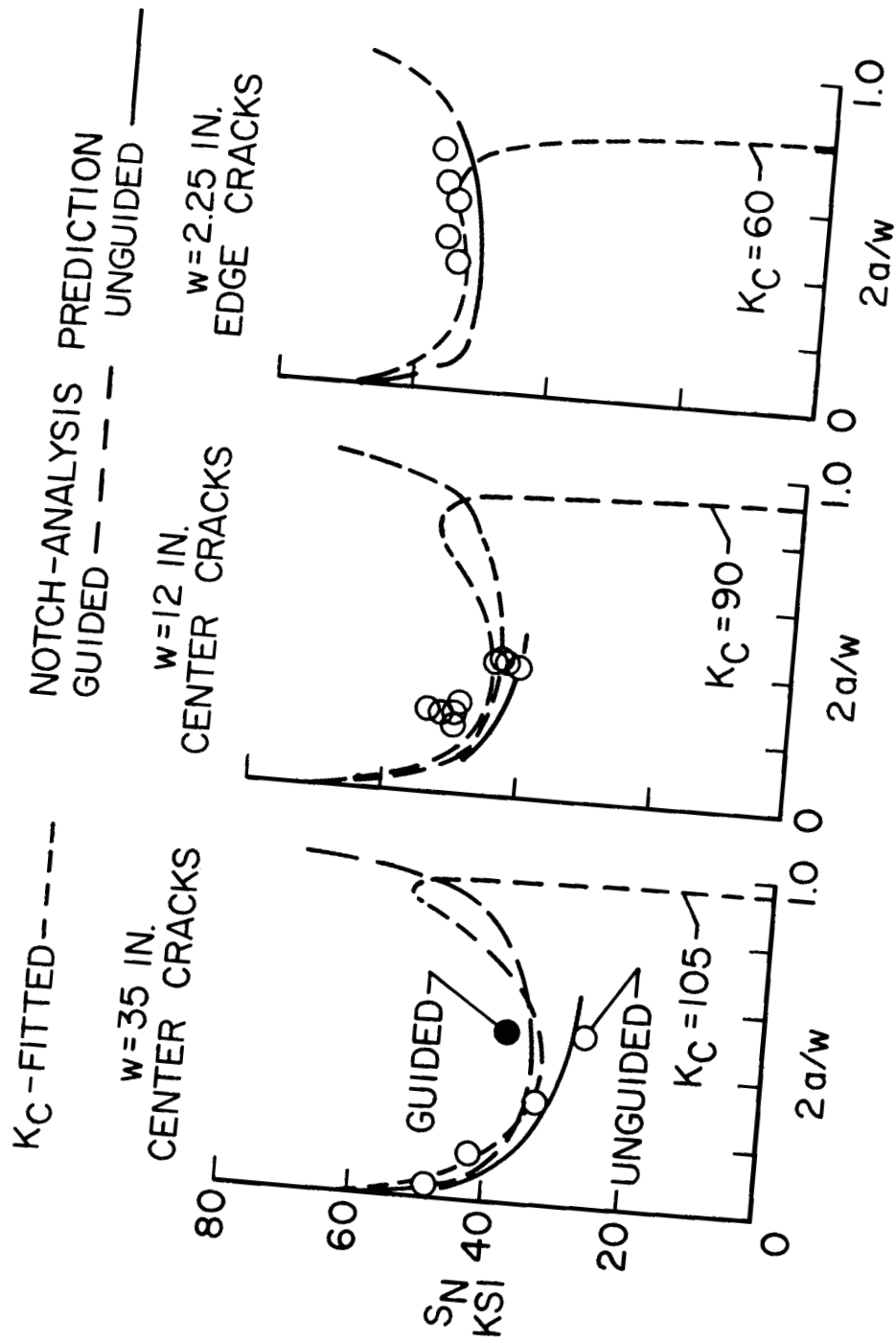
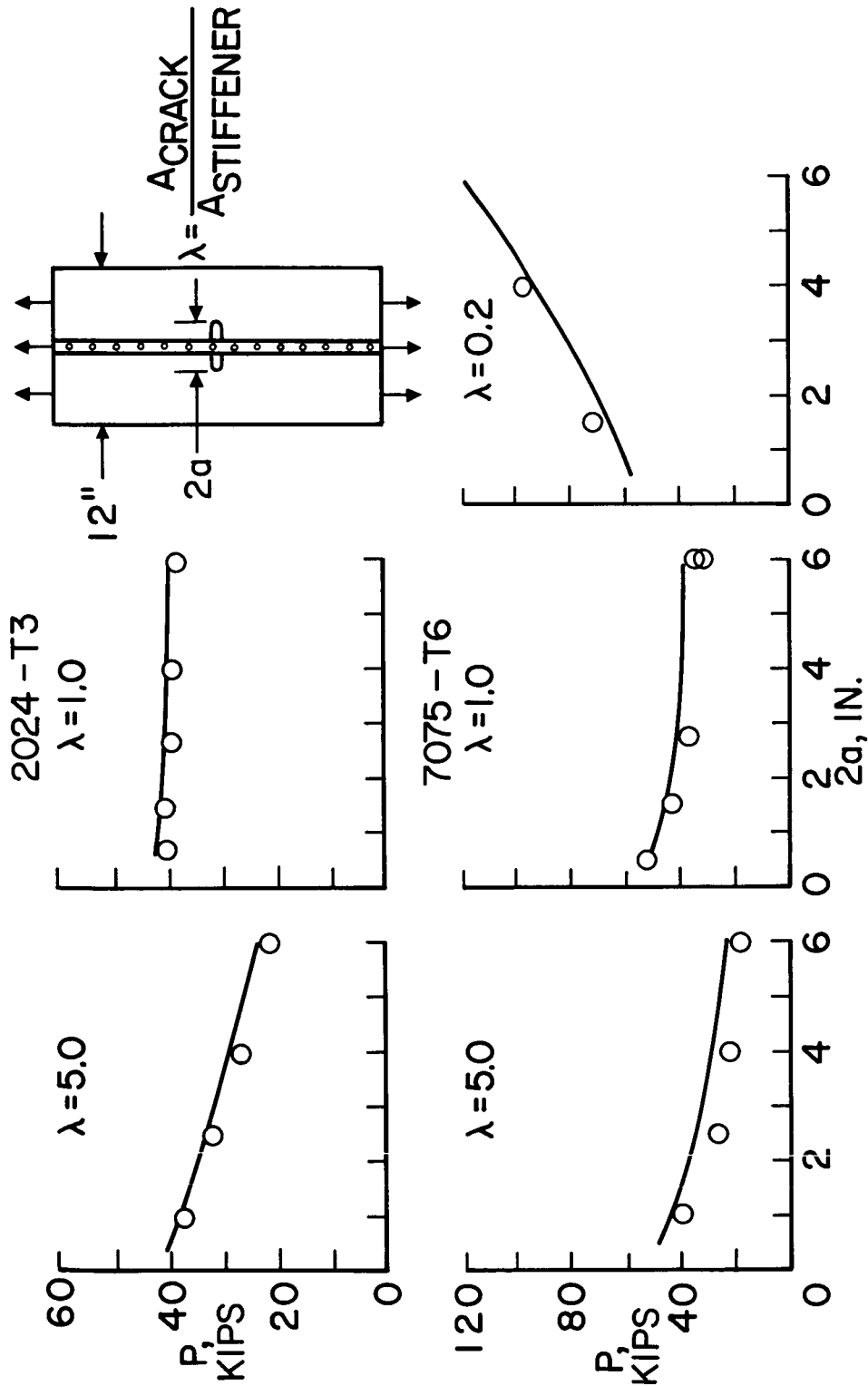
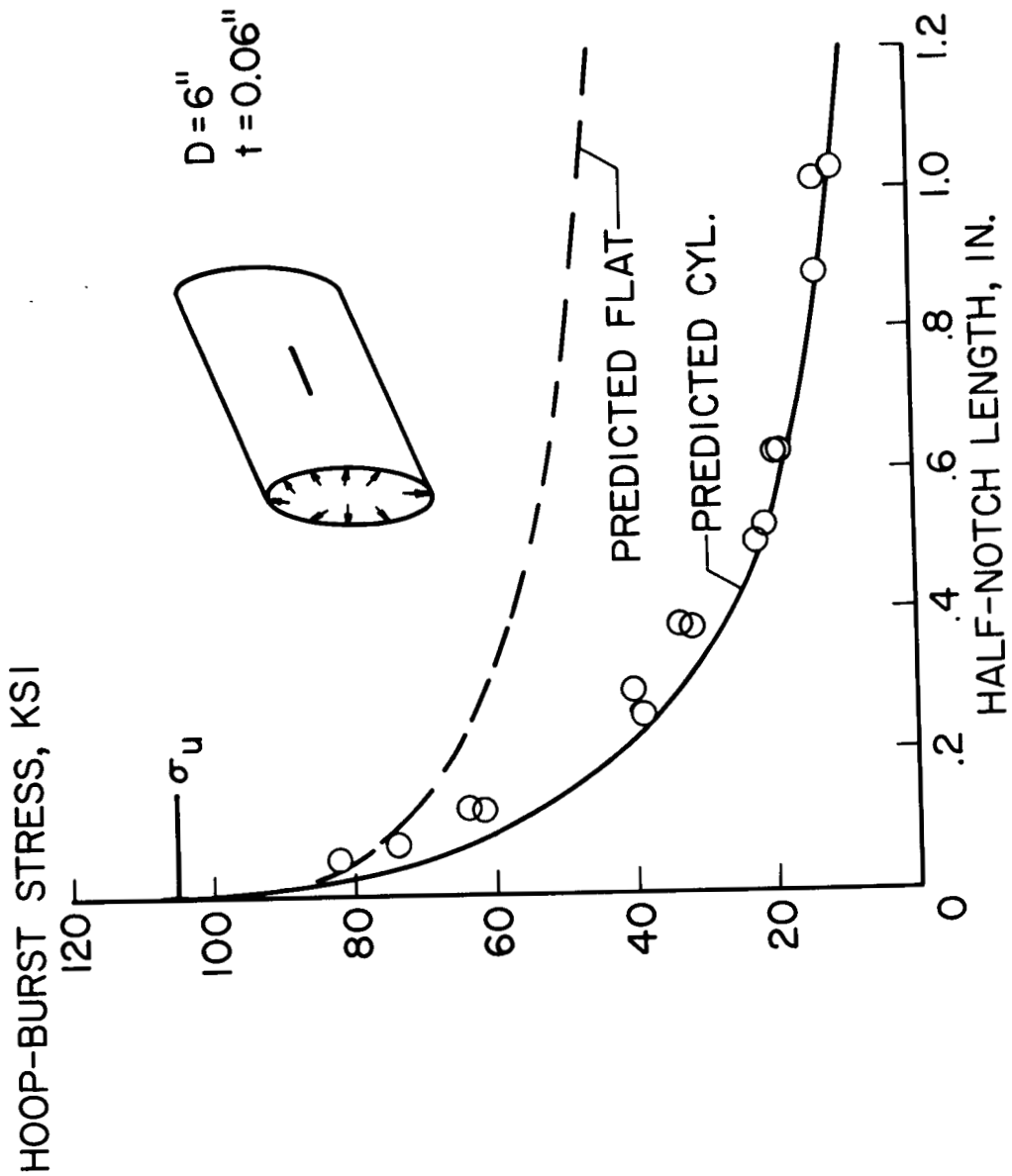


Figure 11.- Crack strength of 2024-T3 aluminum-alloy sheet specimens compared with notch-analysis predictions and  $K_C$  fitted curves.



NASA

Figure 12.- Experimental and predicted failing loads on slotted sheets with stiffeners bridging slots. Data from reference 15.



NASA

Figure 13.- Experimental and predicted bursting stresses on cracked 2014-T6 cylinders. Test data from reference 17.